

The absorption spectrum of hydrogenated silicon carbide nanocrystals from *ab initio* calculations

Márton Vörös,¹ Péter Deák,² Thomas Frauenheim,² and Adam Gali^{3,1}

¹*Department of Atomic Physics, Budapest University of Technology and Economics, Budafoki út 8., H-1111, Budapest, Hungary*

²*Bremen Center for Computational Materials Science,*

Universität Bremen, Otto-Hahn-Allee 1, 28359 Bremen, Germany

³*Department of Physics and School of Engineering and Applied Sciences, Harvard University, Cambridge, Massachusetts 02138, USA*

The electronic structure and absorption spectrum of hydrogenated silicon carbide nanocrystals (SiCNC) have been determined by first principles calculations. We show that the reconstructed surface can significantly change not just the onset of absorption, but the *shape* of the spectrum at higher energies. We found that the absorption threshold of the reconstructed SiCNCs cannot be accurately predicted from traditional density functional theory calculations.

PACS numbers: 78.67.Bf, 73.22.-f, 71.15.Qe

Semiconductor nanocrystals (NC) are objects of intense interest in fields ranging from biology [1] to third generation solar cells [2, 3]. NCs are small pieces of crystal with a surface to volume ratio that is much larger than is typical for bulk crystals. Therefore, understanding the surface states of NCs could be critical in the interpretation of the measurements, or in applications [4]. Pure covalent semiconductor NCs have dangling bonds at the surface that can easily react with the molecules present in the environment. The simplest example is when the dangling bonds are saturated by hydrogen atoms. It is well-known from surface studies of bulk covalent semiconductors that saturation can happen either by conserving the bulk-like structure at the surface or by reconstruction at the surface with formation of long bonds. In what follows, we will refer to a non-reconstructed surface as an “ideal” surface. While the structure of surface reconstruction and its effect on the electrical/optical properties can be monitored by experiments and first principles simulations for the bulk crystals, our understanding of semiconductor NCs remains undeveloped. Traditional *ab initio* density functional theory (DFT) calculations have been successfully applied to explore the geometry and *electronic* structure of small covalent semiconductor NCs, and rarely, up to experimental sizes [5]. However, accurate calculation of the absorption spectrum of NCs requires methods *beyond* DFT that are usually computationally prohibitive. While DFT is a ground state theory, it is usually assumed that one can use the DFT electronic gap [6] with some “rigid shift” to calculate the absorption threshold of the NCs. For example, a difference of ≈ 1.5 eV was deduced by comparing the DFT and Quantum Monte Carlo results on ideal very small hydrogenated silicon nanocrystals [7]. However, it is not clear whether this type of correction may hold for the reconstructed surface. In addition, the surface states may modify not just the absorption threshold of the ideal nanocrystals, but the other part of the spectrum as well.

In this Letter we investigate ideal and recon-

structed hydrogenated cubic silicon carbide nanocrystals (SiCNC). The choice of this material was made for several reasons: i) as a binary compound material one can study the effect of two types of termination ii) SiCNC is one of the most promising candidates for bioinert biomarkers [8, 9, 10] and environmental friendly nanooptics [11, 12, 13] iii) the experimental absorption spectrum is available for small-medium sized colloidal SiCNCs [9]. We determined the structure by standard DFT calculations (PBE) while the absorption spectrum was calculated by hybrid functional based time-dependent DFT (TDPBE0) calculations. We found that i) the TDPBE0 absorption threshold of the ideal SiCNCs is higher than their PBE electronic gap by approximately 1 eV ii) the reconstructed surface can significantly change not just the onset of absorption, but the *shape* of the spectrum at higher energies compared to that of the ideal SiCNCs. Our calculations indicate that not just the position of the absorption threshold but the shape of the absorption spectrum can experimentally discriminate the “ideal”, and the reconstructed, hydrogenated covalent NCs.

Model NCs were constructed by a cutting approximately spherical clusters out of the perfect cubic SiC crystal in such a way that maximum two dangling bonds per surface atoms were allowed. The radii of the resulting clusters are ranged from 0.9 to 2.8 nm. The spherical shape was chosen based on the results of transmission electron microscope measurements (TEM) results [9, 10, 14]. The dangling bonds of the surface atoms were saturated by hydrogen atoms. The geometry of these structures were optimized by using the DFT PBE functional [15]. We will refer to these relaxed NCs as the “ideal” ones. Further relaxation after removing some hydrogen atoms allows the formation of long bonds on the surface. Typically, 2×1 -type reconstruction occurs on the (100) facets but other reconstructions were found as well. For geometry optimization we have utilized the SIESTA code [16] using a double- ζ polarized basis set and Troullier-Martins pseu-

dopotentials [17]. Since SIESTA is a supercell code, at least a distance of 10 Å was ensured between periodic images. All the atoms were allowed to relax until the forces were below 0.02 eV/Å. The $d \approx 1.0$ nm SiCNCs were studied by well converged plane wave calculations [18]. The results agreed within 0.01 Å for the geometries and 0.1 eV for the electronic gaps. Due to the self-interaction error, PBE underestimates the electronic gap, and the best remedy for this problem would be the use of a GW-method [19]. However, GW-method would impose strict limits on the NC size. Instead, a hybrid functional may be applied, since those were shown to reproduce the experimental gap quite well for many different systems [20]. We applied the PBE0 functional to calculate the electronic structure at the PBE geometry [21]. While the electronic gap obtained this way could be rather accurate, the large electron-hole interaction in SiCNCs [22] can reduce the observed “optical” gap in the absorption spectrum considerably. Therefore, we applied time-dependent DFT (TDDFT) with the PBE0 functional in the kernel (TDPBE0), in order to obtain the absorption spectrum of the SiCNCs. We define the exciton binding energy as the difference of the PBE0 electronic gap and the optical gap. *We were able to calculate the absorption spectrum for NCs up to $d \approx 1.5$ nm, i.e., the experimental size range could be reached.* For these calculations the TURBOMOLE cluster code [23] was utilized, applying an all-electron Gaussian basis set with the same quality for the valence electrons as used in the SIESTA code. We used a frequency-domain TDDFT-method, that allowed us to span the selected region of the excitation energy and analyze the nature of the transition [23]. In particular, we determined the application-relevant low energy absorption spectrum for which experimental data are available [9]. Similar hybrid functional based TDDFT-methods yielded superior results for small hydrogen nanoclusters and molecules over TDPBE results, and fairly reproduced the experimental spectrum and/or highly accurate quantum chemistry results [24].

We first considered the ideal SiCNCs. There are two possibilities to construct a spherical NC at any size: a C- and a Si-atom in the center. For instance, an NC with $d \approx 0.9$ nm contains altogether 35 atoms. If Si is at the center, this means 19 Si and 16 C atoms, if C is at the center then the atom counts are reversed. For $d \leq 1.4$ nm, these two types of SiNCs yield considerable difference in both the electronic and optical gaps (see Table I). Generally, the gaps are smaller for those NCs that contain more Si-H than C-H bonds at the surface. For larger NCs the difference is below ≈ 0.2 -0.1 eV.

As apparent from Fig. 1a, there may be strong steric repulsion between some H-atoms on the surface of the ideal NCs. By removing such close H pairs, we allowed the surface to reconstruct while keeping the stoichiometry of the SiCNCs. The steric repulsion is especially strong for the Si-terminated surface. This is expected

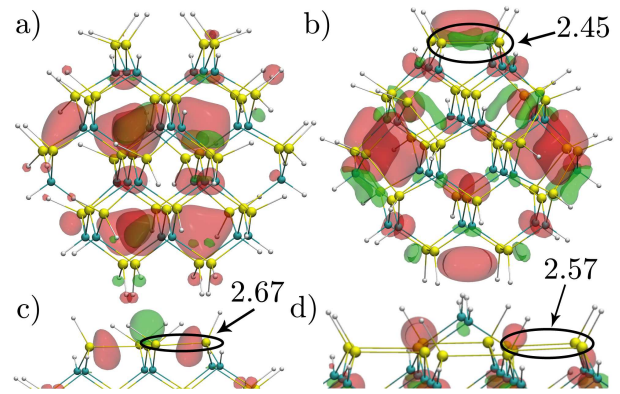


FIG. 1: (Color online) a) The “ideal” $d=1.0$ nm SiCNC, b) typical Si 2×1 -type reconstruction in $d=1.0$ nm SiCNC c) a part of 3×1 -type reconstructions in $d=1.5$ nm SiCNC d) a part of step-like reconstruction in $d=2.1$ nm SiCNC. The bond length of the long Si-Si bonds are shown in Å. Small(big) cyan(yellow) and white balls represent C(Si) and H atoms, respectively. The red(green) lobes show the positive(negative) isosurfaces of the LUMO states.

since the second neighbor distance between the Si-atom is about 3.0 Å in SiC, and the corresponding Si-H bonds are about 1.5 Å. This effect is much less pronounced for the C-terminated surface where the C-H distance is about 1.1 Å. Typically, 2×1 -type reconstructions occurred at the (100) facets (see Fig. 1b), in agreement with previous PBE calculations [11]. In some cases, we have found 3×1 -type (Fig. 1c) and step-like (Fig. 1d) reconstructions at Si-terminated facets. We note that the Si-Si bonds are longer in 3×1 -type and step-like reconstructions than in 2×1 -type reconstructions. The appearance of the 3×1 -type and step-like reconstructions depends strongly on the actual shape of SiCNC surface, and are not as common as the 2×1 -type reconstructions at the Si-terminated (100) facets. If the formation of SiCNCs is driven by kinetics, then in principle any of the surfaces previously discussed could be formed. If SiCNCs are formed at near equilibrium conditions, then 2×1 -type reconstructions could occur most frequently beside the ideal ones [11].

The calculated gaps of the reconstructed SiCNCs can be found in Table I. We also give the calculated TDPBE0 absorption spectrum in Fig. 2, averaged for all the considered SiCNCs by excluding or including the reconstructed NCs. We show the effect of the typical 2×1 -type (Fig. 2b) and the atypical 3×1 -type reconstructions (Fig. 2c) separately. We used Lorentzian broadening of 0.05 eV for each individual peak to construct the spectrum.

Several very important issues can be concluded from Table I and Fig. 2. We first analyze the ideal SiCNCs. In the given size range of the SiCNCs, the electronic gap obtained with PBE0 is about 1.9-1.7 eV larger than the one from PBE, while the difference in optical gaps is about half as large. It should be noted

TABLE I: The atomic structure of the studied ideal and reconstructed SiCNCs and their calculated gaps. First, second and third columns: number of all atoms (#All) with labeling the reconstruction type in parentheses, total number of C and Si atoms (#C,Si), and its diameter (d) in nm. Fourth, fifth and sixth columns: PBE, PBE0 and TDPBE0 gaps in eV, respectively. H \rightarrow L: the contribution of HOMO \rightarrow LUMO transition to the absorption onset in %. Δ_{QP} =PBE0–PBE gaps, i.e., the “quasi-particle” corrections. Δ_{Exc} =TDPBE0–PBE0 gaps, i.e., the binding energy of the exciton. Δ_{Corr} =TDPBE0–PBE gaps. The A/B means the values for Si/C centered SiCNCs, respectively.

#All	#C,Si	d (nm)	PBE(eV)	PBE0(eV)	TDPBE0(eV)	H \rightarrow L(%)	Δ_{QP} (eV)	Δ_{Exc} (eV)	Δ_{Corr} (eV)
71	35	0.9	4.61/4.85	6.48/6.75	5.53/5.83	97/80	1.87/1.90	-0.95/-0.92	0.92/0.98
130	66	1.0	3.79/4.09	5.61/5.91	4.88/5.03	97/97	1.82/1.82	-0.73/-0.88	1.09/0.94
106(2 \times 1)	66	1.0	3.20/3.17	4.87/4.94	4.27/4.13	0/64	1.67/1.77	-0.60/-0.81	1.07/0.96
142	78	1.1	3.81/3.90	5.59/5.69	4.75/4.89	97/94	1.78/1.79	-0.84/-0.81	0.94/0.99
130(2 \times 1)	78	1.1	3.54/3.57	5.33/5.28	4.59/4.69	94/0	1.79/1.71	-0.74/-0.58	1.06/1.13
163	87	1.2	3.66/3.58	5.44/5.35	4.64/4.57	97/94	1.78/1.77	-0.80/-0.79	0.98/0.99
247	147	1.4	3.24/3.30	4.96/5.03	4.22/4.31	96/84	1.72/1.73	-0.74/-0.72	0.98/1.01
223(2 \times 1)	147	1.4	3.11/2.82	4.77/4.55	4.19/4.18	95/0	1.66/1.73	-0.58/-0.37	1.08/1.37
292	172	1.5	3.11/3.06	4.82/4.78	4.11/4.08	96/93	1.71/1.72	-0.71/-0.69	1.00/1.01
292(3 \times 1)	172	1.5	1.96/-	3.51/-	3.10/-	0/-	1.55/-	-0.41/-	1.14/-

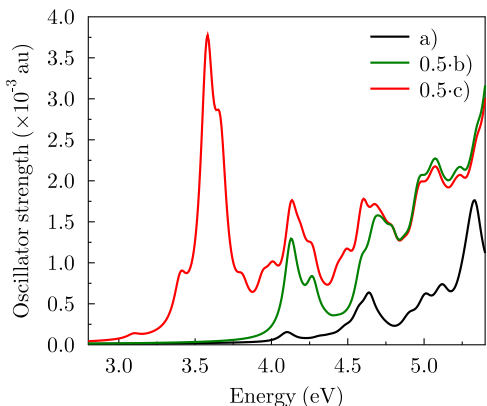


FIG. 2: (Color online) The calculated absorption spectrum of the ensemble of $1.0 \leq d \leq 1.5$ nm SiCNCs a) without b) with 2 \times 1-type reconstructed configurations. c) the same with b) plus 3 \times 1-type reconstruction. b) and c) are scaled by 0.5 as indicated.

that that both the PBE0–PBE difference (corresponding roughly to the necessary quasiparticle correction) and the TDPBE0–PBE0 difference (the binding energy of the exciton) are decreasing continuously with increasing size by approximately the same amount (by about 0.3 eV from $d \approx 0.9$ nm to $d \approx 1.5$ nm). Both effects are understandable, if we consider that by increasing the size of the NCs, the screening is enhanced, reducing the quasiparticle correction, while the HOMO and LUMO wave functions can become more delocalized, increasing the exciton radius. Since the two effects cancel each other almost perfectly, we find that by adding 1.0 eV to the PBE gaps we can reproduce the calculated TDPBE0 optical gaps within 0.09 eV for $0.9 \leq d \leq 1.5$ nm SiCNCs. We note that the first absorption peak is primarily the result of the transition between the HOMO and LUMO states, and therefore the “rigid shift” correction is justified.

The 2 \times 1-type reconstruction causes a large reduction in the optical gap of the $d \approx 1.0$ nm SiCNCs compared to their ideal counterparts, while a small red-shift (≈ 0.2 eV) appears for the larger SiCNCs. This red-shift is associated with the reduced number of Si-H bonds. These findings can be understood, considering that the longer surface Si–Si bonds lead to a smaller bonding-antibonding splitting, and to the appearance of localized surface states in the “bulk” gap of the ideal small SiCNC. As the NC size increases and the bulk gap decreases, these surface states merge with the “bulk”-like states of ideal SiCNCs. For example, the smallest optical gap (3.10 eV), is found for an atypical 3 \times 1-type reconstruction with a very long Si–Si bond. With a single exception, the PBE+1.0 eV \approx TDPBE0 “rule” seems to apply for the reconstructed surfaces, too (see Δ_{Corr} in Table I). However, this is a fortuitous cancellation of errors, since the first absorption peak often does *not* come from the HOMO-LUMO transition: it can be absolutely dark (H \rightarrow L=0 in Table I). Generally, these surface states must be studied one-by-one, and one should not assume a very simple rigid shift correction. The calculated absorption spectrum of the ideal SiCNCs shows an overall monotone increasing function in the given range (see Fig. 2). We found a typical peak at about 4.6 eV due to the wave functions that cause the $\Gamma \rightarrow L$ enhanced absorption at similar energy in bulk cubic SiC. As apparent from Fig. 2, the reconstructed surface *alters not just the absorption treshold but the shape of the spectrum* compared to the ideal NCs. The huge peak at about 3.5 eV comes primarily from 3 \times 1-type reconstructions. The overall larger absorption from the reconstructed surfaces is partly due to the enhanced dipole transition strength between the localized states, and partly due to higher density of states near the gap. For these small/medium SiCNCs the quantum confinement effect can be fully obscured by reconstructed SiCNCs.

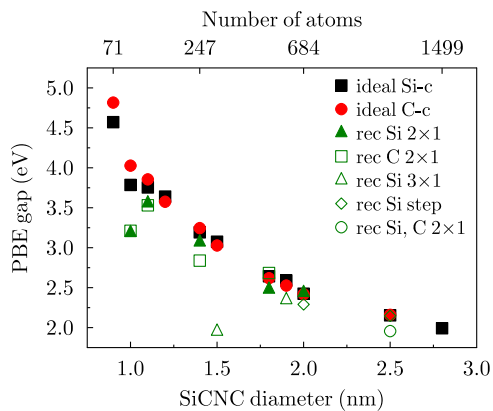


FIG. 3: (Color online) The calculated PBE gap of the ideal and reconstructed SiCNCs. Si-c(C-c) means Si(C) atoms in the center.

We report the PBE electrical gap for large SiCNCs in Fig. 3. Here, we allowed the atypical 3×1 -type or step-like reconstructions together with the typical 2×1 -type reconstruction in the same SiCNC. The trend indicates that the states associated with the atypical reconstructions will merge with the “bulk”-like states of the ideal $d\geq 3$ nm SiCNCs. Therefore, the surface reconstruction does not change the absorption threshold of the ideal counterparts. For the step-like atypical reconstructions (Fig. 1d) we found an enhanced density of states close to HOMO level that may result in somewhat enhanced absorption compared to their ideal counterpart. Nevertheless, the surface to volume ratio grows rapidly with the increasing size of the SiCNCs. Therefore, we predict that the states from surface reconstructions cannot be recognized for $d\geq 3$ nm SiCNCs. We note that Botsoa *et al.* found the first absorption peak at 1.8 eV for colloidal SiCNCs where $d\approx 1.5$ nm SiCNCs were in the vast majority [9]. Another group measured this onset to occur at ≈ 2.75 eV for colloidal $d\approx 3.9\pm 1.1$ nm SiCNCs [10]. This runs against the expected trend of the quantum confinement effect [22] that may be explained by surface reconstructions. However, the onset and the *shape* of our calculated absorption spectrum do not show the features of Botsoa’s experimental data (c.f., Fig. 2a in Ref. 9 and our Figs. 2b,c). We could explain those features by oxygen defects at the surface [25].

In summary, we determined the optical gaps of hydrogenated silicon carbide nanocrystals. We found that the surface reconstruction can play a crucial role for small SiCNCs, and we showed that the onset and the *shape* of the absorption spectrum provide useful method for discriminating between reconstructed and ideal nanocrystals.

AG acknowledges the support from Hungarian OTKA No. K-67886 and the NIIF Supercomputer center grant No. 1090 while MV the support from GE Lighting Hungary. The bilateral support from MTA-DFG No. 194

is acknowledged. The fruitful discussions with Thomas Niehaus and Jan Knaup are appreciated.

-
- [1] X. Michalet, F. F. Pinaud, L. A. Bentolila, J. M. Tsay, S. Doose, J. J. Li, G. Sundaresan, A. M. Wu, S. S. Gambhir, and S. Weiss, *Science* **307**, 538 (2005).
 - [2] I. Gur, N. A. Fromer, M. L. Geier, and A. P. Alivisatos, *Science* **310**, 462 (2005).
 - [3] V. I. Klimov, S. A. Ivanov, J. Nanda, M. Achermann, I. Bezel, J. A. McGuire, and A. Piryatinski, *Nature* **447**, 441 (2007).
 - [4] A. Pandey and P. Guyot-Sionnest, *Science* **322**, 929 (2008).
 - [5] Y. Zhou, Y. Saad, M. L. Tiago, and J. R. Chelikowsky, *Physical Review E* **74**, 066704 (2006).
 - [6] The electronic gap is defined as the difference of the single particle levels of the highest occupied molecular orbital (HOMO) and the lowest unoccupied molecular orbital (LUMO).
 - [7] A. Puzder, A. J. Williamson, J. C. Grossman, and G. Galli, *Phys. Rev. Lett.* **88**, 097401 (2002).
 - [8] Adam Gali’s seminar at the Physics Department of Harvard University (2007, May).
 - [9] J. Botsoa, V. Lysenko, A. Gélóën, O. Marty, J. M. Bluet, and G. Guillot, *Applied Physics Letters* **92**, 173902 (2008).
 - [10] J. Fan, H. Li, J. Jiang, L. K. Y. So, Y. W. Lam, and P. K. Chu, *Small* **4**, 1058 (2008).
 - [11] F. Reboredo, L. Pizzagalli, and G. Galli, *Nano Letters* **4**, 801 (2004).
 - [12] Z. Makkai, B. Pécz, I. Bársony, G. Vida, A. Pongrácz, K. V. Josepovits, and P. Deák, *Applied Physics Letters* **86**, 253109 (2005).
 - [13] X.-H. Peng, S. K. Nayak, A. Alizadeh, K. K. Varanasi, N. Bhate, L. B. Rowland, and S. K. Kumar, *Journal of Applied Physics* **102**, 024304 (2007).
 - [14] X. L. Wu, J. Y. Fan, T. Qiu, X. Yang, G. G. Siu, and P. K. Chu, *Physical Review Letters* **94**, 026102 (2005).
 - [15] J. P. Perdew, K. Burke, and M. Ernzerhof, *Phys. Rev. Lett.* **77**, 3865 (1996).
 - [16] J. M. Soler, E. Artacho, J. D. Gale, A. García, J. Junquera, P. Ordejón, and D. Sánchez-Portal, *Journal of Physics: Condensed Matter* **14**, 2745 (2002).
 - [17] N. Troullier and J. L. Martins, *Phys. Rev. B* **43**, 1993 (1991).
 - [18] For this purpose the PWSCF code (P. Giannozzi *et al.*, <http://www.quantum-espresso.org>) was applied with using standard ultrasoft pseudopotentials and 40 Ry plane wave cut-off.
 - [19] L. Hedin and S. Lundqvist, in *Solid State Physics*, edited by H. Ehrenreich, F. Seitz, and D. Turnbull (Academic, New York, 1969), Vol. 23.
 - [20] M. Marsman, J. Paier, A. Stroppa, and G. Kresse, *Journal of Physics: Condensed Matter* **20**, 064201 (9pp) (2008).
 - [21] J. P. Perdew, M. Ernzerhof, and K. Burke, *Journal of Chemical Physics* **105**, 9982 (1996).
 - [22] D. H. Feng, Z. Z. Xu, T. Q. Jia, X. X. Li, and S. Q. Gong, *Phys. Rev. B* **68**, 035334 (2003).
 - [23] R. Bauernschmitt and R. Ahlrichs, *Chem. Phys. Letters*

- 256**, 454 (1996).
- [24] O. Lehtonen and D. Sundholm, *Physical Review B* **74**, 045433 (2006).
- [25] M. Vörös, P. Deák, T. Frauenheim, and A. Gali, unpublished.